Light Higgsino scenario confronted with the muon $g-2$

Jun Zhao,[1,*] Jingya Zhu,[1,†] Pengxuan Zhu,[2,‡] and Rui Zhu[2,3,§]

[1]*Joint Research Center for Theoretical Physics, School of Physics and Electronics, Henan University, Kaifeng 475004, People's Republic of China*

[2]*CAS Key Laboratory of Theoretical Physics, Institute of Theoretical Physics, Chinese Academy of Sciences, Beijing 100190, People's Republic of China*

[3]*School of Physics Sciences, University of Chinese Academy of Sciences, Beijing 100049, People's Republic of China*

(Received 5 December 2022; accepted 27 February 2023; published 21 March 2023)

Light Higgsinos below several hundred GeV are favored or required by the naturalness of low-energy supersymmetry. If only Higgsinos are light while other sparticles are sufficiently heavy, we have the so-called light Higgsino scenario. Confronted with the muon $g-2$ data, this scenario is examined in this work. Since in this scenario the lightest sparticle is Higgsino-like, we need to also consider the dark matter constraints. Assuming a light Higgsino mass parameter μ in the range of 100–400 GeV while gaugino mass parameters above TeV, we explore the parameter space under the muon $g-2$ data and the dark matter constraints. We find that, to explain the muon $g-2$ anomaly at 2σ, the winos and sleptons are, respectively, upper bounded by 3 TeV and 800 GeV. In this case, we find that the light Higgsino-like dark matter can sizably scatter with nucleon and thus the allowed parameter space can be covered almost fully by the future LZ dark matter detection project. We also perform a Monte Carlo simulation to figure out the potential of High-Luminosity Large Hadron Collider (HL-LHC) to detect the light sleptons in this scenario. It turns out that compared with the current LHC limits, the HL-LHC can further cover a part of the parameter space.

DOI: 10.1103/PhysRevD.107.055030

I. INTRODUCTION

The latest Fermilab result of muon $g-2$ [1], combined with the BNL result [2], is 4.2σ above the SM prediction [3,4]; i.e., the experimental value exceeds the SM value by $(2.51 \pm 0.59) \times 10^{-9}$. For new physics researchers, this anomaly is just like when a long drought meets a shower of rain. As said by Steven Weinberg forty years ago, "Physics thrives on crisis. We all recall the great progress made while finding a way out of the various crises of the past [5]." Now to move on beyond the Standard Model (SM) we indeed need a crisis from experiments. Such an anomaly from the muon $g-2$ measurement may serve as a crisis (albeit some lattice calculations [6–10] seem to shift up the SM value to relax this crisis, which, however, may transfer the crisis to the electroweak fit [11–14]) and suggest the direction of new physics. Not surprisingly, this muon $g-2$ anomaly caused a sensation in high energy physics and attempts to explain have been made in various new physics theories.

As a leading new physics candidate, the low-energy supersymmetry (SUSY) has been recently revisited (for recent brief reviews, see, e.g., [15–17]) to explain the muon $g-2$ anomaly; albeit the SUSY contribution was calculated long ago [18–20]. (i) In the low-energy effective SUSY models, such as the minimal supersymmetric model (MSSM) [21,22] and the next-to-minimal supersymmetric model (NMSSM) [22–24], the explanation of the muon $g-2$ anomaly can be readily achieved [25–44]. Also, the explanation can be made in other extensions of the MSSM [45–52]. (ii) The SUSY models with boundary conditions at some high energy scale, such as the CMSSM or mSUGRA, cannot explain the muon $g-2$ anomaly because of the correlation between the masses of the sparticles [35,53,54]. In order to accommodate the muon $g-2$, extensions are needed, such as extending mSUGRA to gluino-SUGRA [55–60], extending gauge-mediated supersymmetry breaking (GMSB) by introducing Higgs-messenger coupling [61,62] or deflecting anomaly mediated supersymmetry breaking (AMSB) [63,64], the flipped $SU(5)$ intersecting D-branes model [65].

Note that in these SUSY explanations of the muon $g-2$, the lightest sparticle (LSP) as the dark matter candidate is usually assumed to be binolike due to the limits from the relic density and direct detections of dark matter.

*junzhao@henu.edu.cn
†zhujy@henu.edu.cn
‡zhupx99@icloud.com
§zhurui@itp.ac.cn

Very recently, the wino-Higgsino admixture, with both winos and Higgsinos below several hundred GeV, was considered as the dark matter candidate to explain the muon $g-2$ anomaly [66], where it was found that the favored parameter space in the spontaneously broken SUGRA is detectable in the future dark matter direct detections or the LHC searches for the electroweakinos. In this work, we will examine another fascinating scenario, the so-called light Higgsino scenario, for the explanation of the muon $g-2$ anomaly. In this scenario only Higgsinos are light, with the Higgsino mass parameter μ being usually in the range of 100–300 GeV, favored or required by the naturalness of SUSY (see, e.g., [67]). This scenario provides a Higgsino-like dark matter (since gauginos are above TeV, significantly heavier than Higgsinos), differing from the scenario with wino-Higgsino admixture as the dark matter considered in [66]. In our study, assuming a light Higgsino mass parameter μ in the range of 100–400 GeV while gaugino mass parameters are above TeV, we will explore the parameter space by considering the muon $g-2$ data and the dark matter constraints. Then for the favored parameter space we will check the detectability of future dark matter detection projects and the High-Luminosity Large Hadron Collider (HL-LHC).

This work is organized as follows. In Sec. II we provide a brief description for the light Higgsino scenario. In Sec. III we perform a numerical scan to locate the parameter space for the explanation of the muon $g-2$ anomaly at 2σ level. In Sec. IV we perform a Monte Carlo simulation to show the HL-LHC detectability for the parameter space favored by the muon $g-2$. Finally, we conclude in Sec. V.

II. A BRIEF DESCRIPTION OF LIGHT HIGGSINO SCENARIO

From the naturalness of SUSY, the Higgsino mass parameter μ cannot be heavy, which can be seen from the following minimization relation of the tree-level Higgs potential [68]:

$$\frac{m_Z^2}{2} = -\mu^2 + \frac{M_{H_d}^2 - M_{H_u}^2 \tan^2\beta}{\tan^2\beta - 1}, \tag{2.1}$$

with $M_{H_d}^2$ and $M_{H_u}^2$ being the soft SUSY breaking masses of the Higgs fields at weak scale, while μ is the mass parameter of the Higgsinos. Obviously, the value of μ cannot be too large compared with the weak scale in order to avoid fine-tuning, which in natural SUSY [67] is assumed to be smaller than 300 GeV. Since naturalness has no strict criterion, we, in this work, assume μ in the range of 100–400 GeV.

In the light Higgsino scenario, the gauginos are heavy (above TeV) and thus the LSP as the dark matter candidate is utterly dominated by Higgsinos. Not only is the LSP Higgsino-like, but the next-to-lightest sparticles (the neutralino $\tilde{\chi}_2^0$ and chargino $\tilde{\chi}_1^\pm$) are also Higgsino-like, all of which are nearly degenerate, having a mass around the value of μ. These Higgsino-dominated electroweakinos are approximately given as follows [49]:

$$m_{\tilde{\chi}_1^\pm} \sim \mu, \qquad m_{\tilde{\chi}_{1,2}^0} = \mu \mp \Delta m,$$
$$\Delta m \simeq \frac{g_1^2 v^2 M_1}{M_1^2 - \mu^2} + \frac{g_2^2 v^2 M_2}{M_2^2 - \mu^2}, \tag{2.2}$$

with $v = 246$ GeV being the Higgs vacuum expectation value, M_1 and M_2 being the soft SUSY breaking masses of bino and wino fields, respectively. When M_1 and M_2 are both greater than 1 TeV, the mass splitting Δm is less than 1 GeV. In this case, since the visible particles from the Higgsino decay are too soft, the productions of these Higgsino-like sparticles at the colliders merely give missing energy and can only be detected by requiring one initial state radiation (ISR) jet, e.g., at the LHC the signal of monojet plus missing energy [69]. Since such productions of Higgsino-like electroweakinos are proceeded by electroweak interaction, a global likelihood analysis showed that no clear range of their masses can be robustly excluded by current LHC searches [70]. Very recently, the LHC constraints on the electroweakinos were revisited [71], which showed that these Higgsino-like electroweakinos as light as 100 GeV are still allowed.

Since in this scenario gauginos are heavy (above TeV), the LSP as a dark matter candidate is dominated by light Higgsinos. Such light Higgsino-like LSPs can efficiently annihilate, e.g., through the s-channel Z-boson exchange, to have a large annihilation rate in the early Universe. Thus they usually give a thermal relic density under abundance. This implies that these light Higgsino-like LSPs are only a component of dark matter while other components like axions are needed. Therefore, in this scenario the LSP-nucleon scattering cross section must be rescaled by a factor $\Omega_{\rm LSP}h^2/\Omega_{\rm PL}h^2$, with $\Omega_{\rm PL}h^2$ being the observed relic density by Planck satellite.

III. PARAMETER SPACE FOR MUON $g-2$

In our scan, we assume light Higgsinos and heavy gauginos

$$100\ \text{GeV} \le \mu \le 400\ \text{GeV}, \qquad 1\ \text{TeV} \le M_1, \qquad M_2 \le 5\ \text{TeV}. \tag{3.1}$$

Since the muon $g-2$ is also sensitive to slepton masses, we scan over it from 200 GeV to 2 TeV

$$200\ \text{GeV} \le M_{L_\ell} = M_{E_\ell} \le 2\ \text{TeV}, \tag{3.2}$$

where $\ell = e,\ \mu$. For the third-generation squark mass parameters, we require them to be heavy due to the 125 GeV Higgs boson mass

$$3\ \text{TeV} \le M_{Q3}, \qquad M_{U3} \le 5\ \text{TeV}. \tag{3.3}$$

For the third-generation sfermion trilinear couplings, we require them in the range

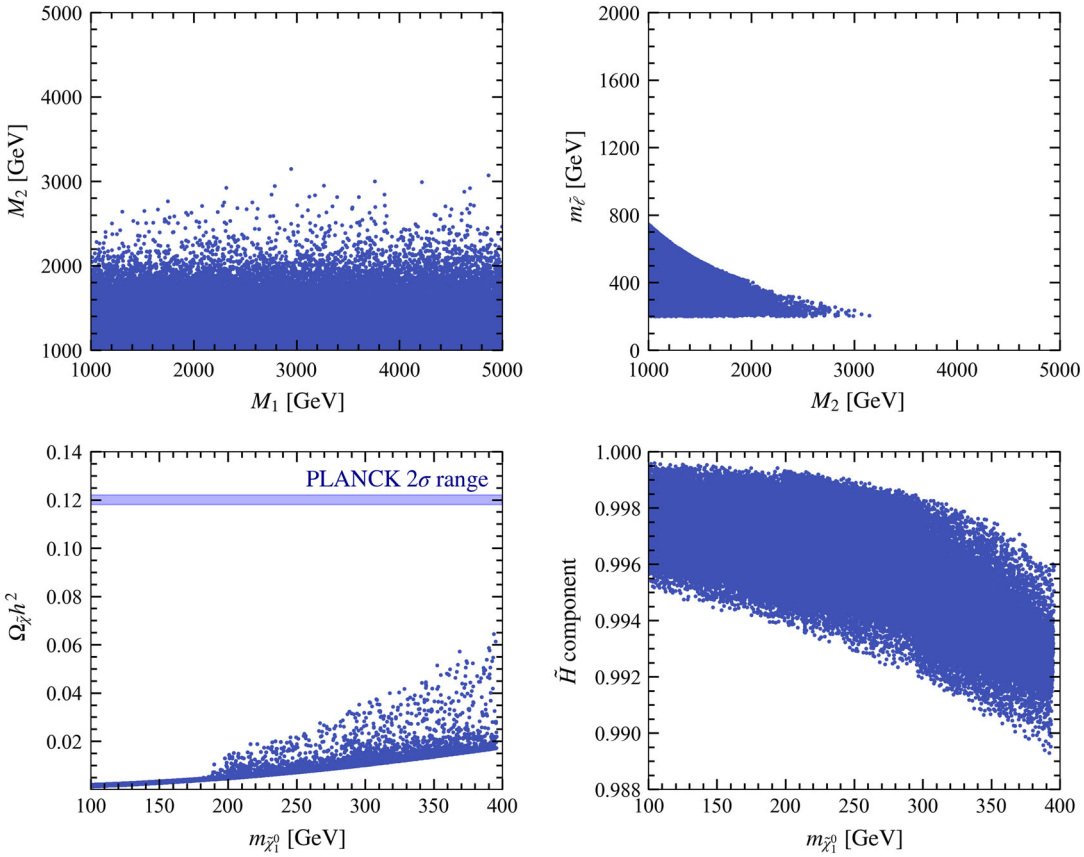

FIG. 1. Scatter plots of the samples that survived the constraints (1–5) including especially the muon $g-2$ at 2σ level.

$$-3\ \text{TeV} \leq A_{t,b,\tau} \leq 3\ \text{TeV}. \tag{3.4}$$

For the value of $\tan\beta$, we scan over it in the range of $1 \leq \tan\beta \leq 50$. Other soft mass parameters are fixed at 5 TeV except for the trilinear ones like $A_{u,d,e}$ which are set to zero. In our scan we consider the following experimental constraints:

(1) The package SUSY-HIT [72] is used for generating the particle spectrum, where the mass spectrum is calculated by subprogram SuSpect-2.41, and the decays of the Higgs boson and sparticles are calculated by subprogram HDECAY-3.4 and SDECAY-1.5, respectively. The Higgs boson masses are evaluated with two-loop corrections, under the approximations of vanishing external momenta and of vanishing electroweak (EW) gauge couplings. So the SM-like Higgs boson mass is required in the range of $122 < m_h < 128$ GeV.[1]

(2) We consider the constraint of metastability of the vacuum state, which requires $|A_t| \lesssim 2.67(m^2_{\tilde{t}_L} + m^2_{\tilde{t}_R} + \mu^2 + m^2_{H_u})$ [81].

(3) The sleptons are required to be above 200 GeV, considering the LEP2 plus LHC constraints.

(4) The LSP dark matter relic density is calculated by micrOMEGAs-5.2.13 [82] and is required below its 2σ upper bound of the Planck observed value $\Omega_{\rm DM}h^2 = 0.120 \pm 0.001$ [83].

(5) The two-loop level SUSY contributions to muon $g-2$ are calculated by the package GM2Calc-2.1.0 [84,85]. We require SUSY to explain the current data $\Delta a_\mu \equiv a_\mu^{\rm exp} - a_\mu^{\rm SM} = (2.51 \pm 0.59) \times 10^{-9}$ [86] within the 2σ range.

In Fig. 1 we plot the scatter plots of the samples survived the constraints (1–5) including especially the muon $g-2$ at 2σ level. This figure shows the following characteristics:

(i) From the top panels we see that in this light Higgsino scenario the muon $g-2$ data at 2σ level requires the wino mass M_2 below 3 TeV and the slepton mass below 800 GeV, while it is not sensitive to the bino mass M_1.

(ii) From the bottom-left panel we see that such Higgsino-like LSP gives a thermal relic density much below the measured abundance.

[1]The accuracy of the Higgs mass calculation has been improved to state of the art. Now the theoretical uncertainties are understandable, and in most recent studies, the total Higgs mass uncertainty was improved to less than 2 GeV for low-energy MSSM parameter space. For the relevant studies, see, e.g., [73–80]. In this work, we adopted 3 GeV as the accuracy in the code SuSpect.

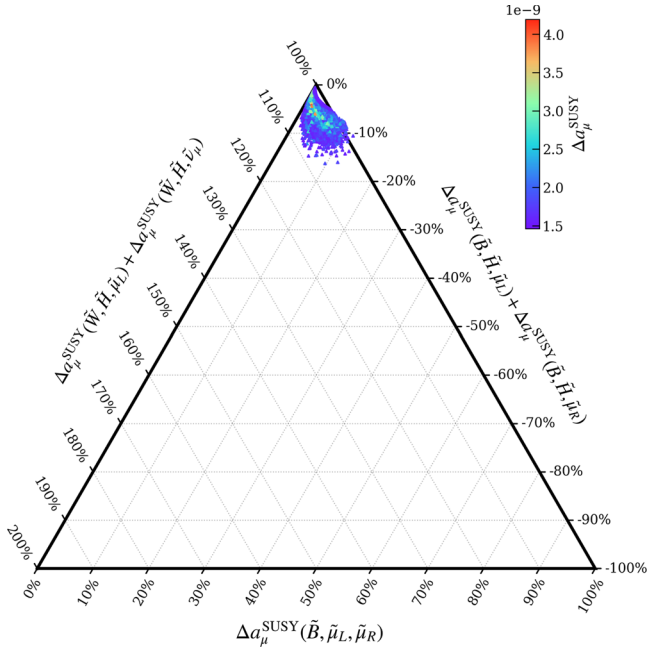

FIG. 2. A ternary plot showing the components of the one-loop SUSY contributions to muon $g-2$. The left axis represents the wino-Higgsino loop, the right axis represents the bino-Higgsino loops, and the bottom axis represents the bino-smuon loop. The colors are coded by the two-loop result of $\Delta a_\mu^{\rm SUSY}$.

(iii) From the bottom-right panel we see the LSP is utterly dominated by the Higgsino component.

The relevant SUSY parameters result in different contributions to $a_\mu^{\rm SUSY}$. The two-loop expressions of $a_\mu^{\rm SUSY}$ implemented in the package GM2Calc take the form in Refs. [87–89]. To figure out the dominant SUSY contribution, the detailed five contributions at one-loop level are shown in Fig. 2 via a ternary scatter plot[2] with the colors coded by $\Delta a_\mu^{\rm SUSY}$. As shown in Fig. 2, the five contributions are classified into three classes: the wino-Higgsino loops $\Delta a_\mu^{\rm SUSY}(\tilde{W},\tilde{H},\tilde{\mu}_L)+\Delta a_\mu^{\rm SUSY}(\tilde{W},\tilde{H},\tilde{\nu}_\mu)$ (left axis), the bino-Higgsino loops $\Delta a_\mu^{\rm SUSY}(\tilde{B},\tilde{H},\tilde{\mu}_L)+\Delta a_\mu^{\rm SUSY}(\tilde{B},\tilde{H},\tilde{\mu}_R)$ (right axis), and the bino-smuon loops $\Delta a_\mu^{\rm SUSY}(\tilde{B},\tilde{\mu}_L,\tilde{\mu}_R)$ (bottom axis). From Fig. 2, one can find the dominant SUSY contribution is from wino-Higgsino loop. The bino-Higgsino loop provides a $\sim 10\%$ negative contribution while the bino-smuon loop provides a $\sim 10\%$ positive contribution.

Therefore, we can understand why a sizable contribution to the muon $g-2$ in this light Higgsino scenario needs a not-too-heavy wino mass. If gauginos are too heavy and decoupled, the light electroweakinos will be only Higgsinos. The interactions of a Higgsino with muon and slepton (smuon or sneutrino) are kinds of Yukawa couplings, which always flip the chirality between muon and slepton. Hence, a pure Higgsino cannot flip the muon chirality via loops, except with a mass insertion of left-right handed smuon transition $m_\mu(A_\ell-\mu\tan\beta)$, which can be neglected. As a result, the pure Higgsinos cannot make enough contributions to explain the muon $g-2$ at 2σ level. When not-too-heavy winos come into play, we have Fig. 3. In this figure, the wino-Higgsino loop contributions are given as follows [18–20,84]:

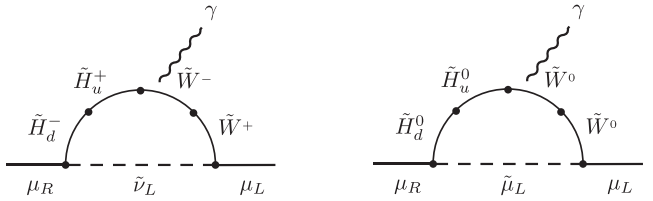

FIG. 3. The muon $g-2$ Feynman diagrams showing the contributions of light Higgsinos assisted by not-too-heavy winos. Here the charged-current loop dominates the contributions.

$$\Delta a_\mu^{\rm SUSY}(\tilde{W},\tilde{H},\tilde{\nu}_\mu)\simeq\frac{g_2^2 m_\mu^2}{8\pi^2}\frac{M_2\mu\tan\beta}{m^4_{\tilde{\nu}_\mu}}\cdot F_a\left(\frac{M_2}{m_{\tilde{\nu}_\mu}},\frac{\mu}{m_{\tilde{\nu}_\mu}}\right),$$
$$\Delta a_\mu^{\rm SUSY}(\tilde{W},\tilde{H},\tilde{\mu}_L)\simeq-\frac{g_2^2 m_\mu^2}{16\pi^2}\frac{M_2\mu\tan\beta}{m^4_{\tilde{\mu}_L}}\cdot F_b\left(\frac{M_2}{m_{\tilde{\mu}_L}},\frac{\mu}{m_{\tilde{\mu}_L}}\right), \tag{3.5}$$

where the loop functions are defined as

$$F_a(x,y)=\frac{1}{2}\frac{G_3(x^2)-G_3(y^2)}{x^2-y^2},$$
$$F_b(x,y)=-\frac{1}{2}\frac{G_4(x^2)-G_4(y^2)}{x^2-y^2},$$
$$G_3(x)=\frac{3-4x+x^2+3\log x}{(1-x)^3},$$
$$G_4(x)=\frac{1-x^2+2x\log x}{(1-x)^3}. \tag{3.6}$$

They satisfy $0\le F_{a,b}(x,y)\le 1$ and are monochromatically increasing for x and y, satisfying $F_a(1,1)=1/2$ and $F_b(1,1)=1/6$ for degenerate sparticle masses.[3] Other contributions come from the bino loops, where the bino-Higgsino loops take approximate forms [18–20,84]

$$\Delta a_\mu^{\rm SUSY}(\tilde{B},\tilde{H},\tilde{\mu}_L)\simeq\frac{g_1^2 m_\mu^2}{16\pi^2}\frac{M_1\mu\tan\beta}{m^4_{\tilde{\mu}_L}}\cdot F_b\left(\frac{M_1}{m_{\tilde{\mu}_L}},\frac{\mu}{m_{\tilde{\mu}_L}}\right),$$
$$\Delta a_\mu^{\rm SUSY}(\tilde{B},\tilde{H},\tilde{\mu}_R)\simeq-\frac{g_1^2 m_\mu^2}{8\pi^2}\frac{M_1\mu\tan\beta}{m^4_{\tilde{\mu}_R}}\cdot F_b\left(\frac{M_1}{m_{\tilde{\mu}_R}},\frac{\mu}{m_{\tilde{\mu}_R}}\right), \tag{3.7}$$

[2]A ternary plot depicts the ratios of the three variables as positions in an equilateral triangle. Note that any one of the variables is not independent to the others.

[3]F_a and F_b are reduced from the functions in Ref. [18].

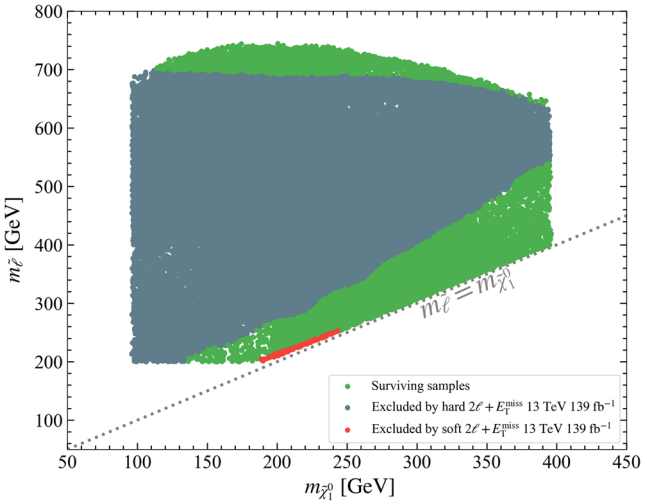

FIG. 4. Same as Fig. 1, but displayed on the plane of slepton mass versus the LSP mass. The regions excluded by the ATLAS searches for the hard dilepton plus missing energy [90] and soft dilepton plus missing energy [91] are shown.

From Eqs. (3.5) and (3.7), one can find that the contributions of the wino-Higgsino loops are positive while the contributions of the bino-Higgsino loops tend to be negative. Since bino in this work is heavier than 1 TeV and its contribution is proportional to g_1^2, about a quarter of g_2^2, so a not-too-heavy bino cannot play a dominated role.

In Fig. 4 we show the samples survived the constraints (1–5) on the plane of slepton mass versus the LSP mass. The regions excluded by the ATLAS searches for the two hard leptons plus missing energy [90] and two soft leptons plus missing energy [91] are displayed. We see that for a large mass splitting between slepton mass and LSP mass, the ATLAS searches for the two hard leptons plus missing energy have excluded a quite large part of the parameter space required for the explanation of the muon $g-2$ at 2σ level. While for a compressed slepton-LSP spectrum, i.e., a very small mass splitting between slepton mass and LSP mass, the exclusion ability of the current LHC is rather limited.

In Fig. 5, we replot the samples of Fig. 4, showing the spin-independent and spin-dependent LSP-nucleon scattering cross sections and the velocity-averaged DM annihilation cross section versus the LSP mass. In the aspect of DM direct detections, the current direct detection limits are shown assuming that a single dark matter candidate constitutes the entire relic. Since the Higgsino-like LSP is underabundant, so the direct detection limits are applied on the scaled cross sections, where the scaling factor is $\Omega_{\rm LSP}h^2/0.12$. We see that after scaling, the most samples of the Higgsino-like LSP can survive the current direct detection limits, while the future LZ-projected can almost cover all the survived samples. Most of the DM indirect detection experiments are searching for the DM self-annihilation rate Γ_A given by

$$\Gamma_A \propto \langle \sigma v \rangle \times \frac{\rho_{\rm DM}^2}{m_{\rm LSP}^2}, \tag{3.8}$$

where $\rho_{\rm DM}$ is the DM density in the local halo. We checked that Higgsino-like LSPs mostly annihilate into gauge bosons (over 80% in most case) and/or Higgs bosons. These primal annihilation products subsequently decayed and can act as the sources of some cosmic ray flux, such as positrons, antiprotons and photons, and neutrino flux in our galaxy. From Fig. 5, one can find that the annihilation rate is diluted by the square of the local density scaling factor. The current experiments, e.g., the constraints from AMS-02 [92], are hard to detect $\langle \sigma v \rangle$ below 10^{-26} cm^3 s^{-1} for $m_{\tilde{\chi}_1^0}$ larger than 100 GeV. Although the limits in Fig. 5 depend on the properties of the DM halo and the cosmic ray propagation, etc., one can argue that the current DM indirect detection experiments are not sensitive to the light Higgsino scenario.

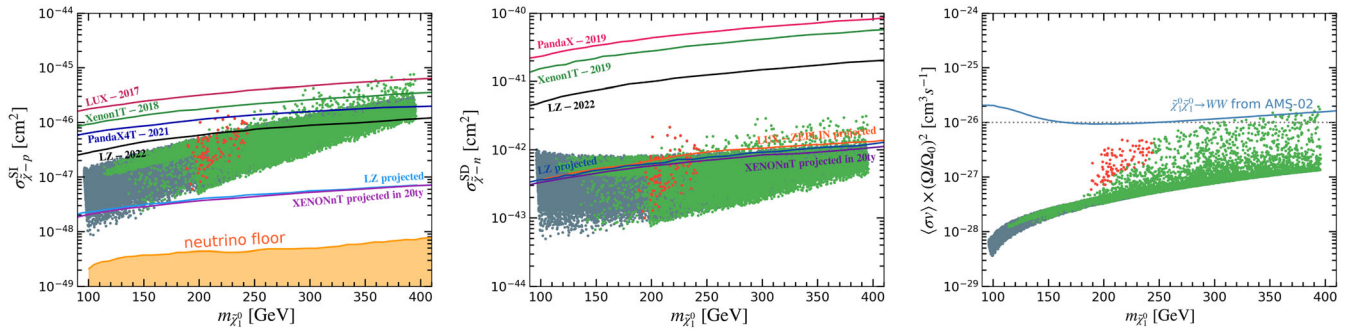

FIG. 5. Same as the samples in Fig. 4, but showing the spin-independent and spin-dependent LSP-nucleon scattering cross sections and DM annihilation cross sections versus the LSP mass. Since the Higgsino-like LSP is underabundant, a scaling factor $\Omega_{\rm LSP}h^2/0.12$ is applied on the LSP-nucleon scattering cross sections. The 90% C.L. upper limits from LUX-2017 [93], XENON1T-2018 [94], XENON1T-2019 [95], PandaX-2019 [96], PandaX4T-2021 [97], LZ-2022 [98] as well as the future sensitivities from LZ [99], XENONnT(20ty) [100] are shown. The 95% C.L. constraints on DM annihilation into WW are derived from the antiproton and B/C data of AMS-02 [92].

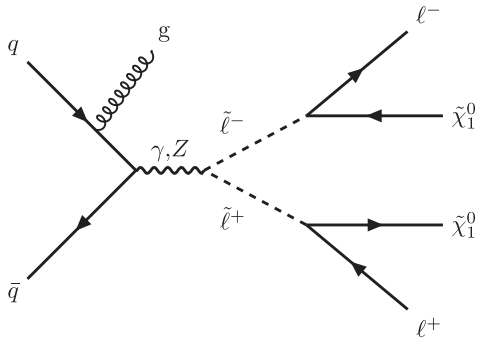

FIG. 6. A typical Feynman diagram for the slepton pair production process $pp \to j\tilde{\ell}^+(\to \ell^+\tilde{\chi}_1^0)\tilde{\ell}^-(\to \ell^-\tilde{\chi}_1^0) \to j + \ell^+\ell^- + E_{\mathrm{T}}^{\mathrm{miss}}$ at the LHC.

IV. DETECTABILITY AT THE HL-LHC

Since the muon $g-2$ data requires sleptons below 800 GeV, we examine the observability of the slepton pair production at the 14 TeV HL-LHC with 3000 fb^{-1}. For this end, we perform a detailed Monte Carlo simulation for the process

$$pp \to j\tilde{\ell}^+(\to \ell^+\tilde{\chi}_1^0)\tilde{\ell}^-(\to \ell^-\tilde{\chi}_1^0) \to j + \ell^+\ell^- + E_{\mathrm{T}}^{\mathrm{miss}}. \tag{4.1}$$

A typical Feynman diagram of this process is shown in Fig. 6. The main SM backgrounds come from the Drell-Yan, dibosons, Z-boson plus jets, and the leptonic top pair events. We use MadGraph5_aMC@NLO [101] to generate parton-level events and then pass the events to PYTHIA [102] for showering and hadronization. We simulate the detector effects by Delphes [103] and perform the analysis of events with CheckMATE2 [104–106]. Finally, the significance is obtained by

$$Z = \frac{S}{\sqrt{S + B + (\beta B)^2}}, \tag{4.2}$$

with S (B) being the events number of signal (SM background) and β being the total systematic uncertainty, taken as $\beta = 10\%$ in our calculations.

Fig. 7 displays the normalized distributions of the missing transverse energy and the dilepton invariant mass

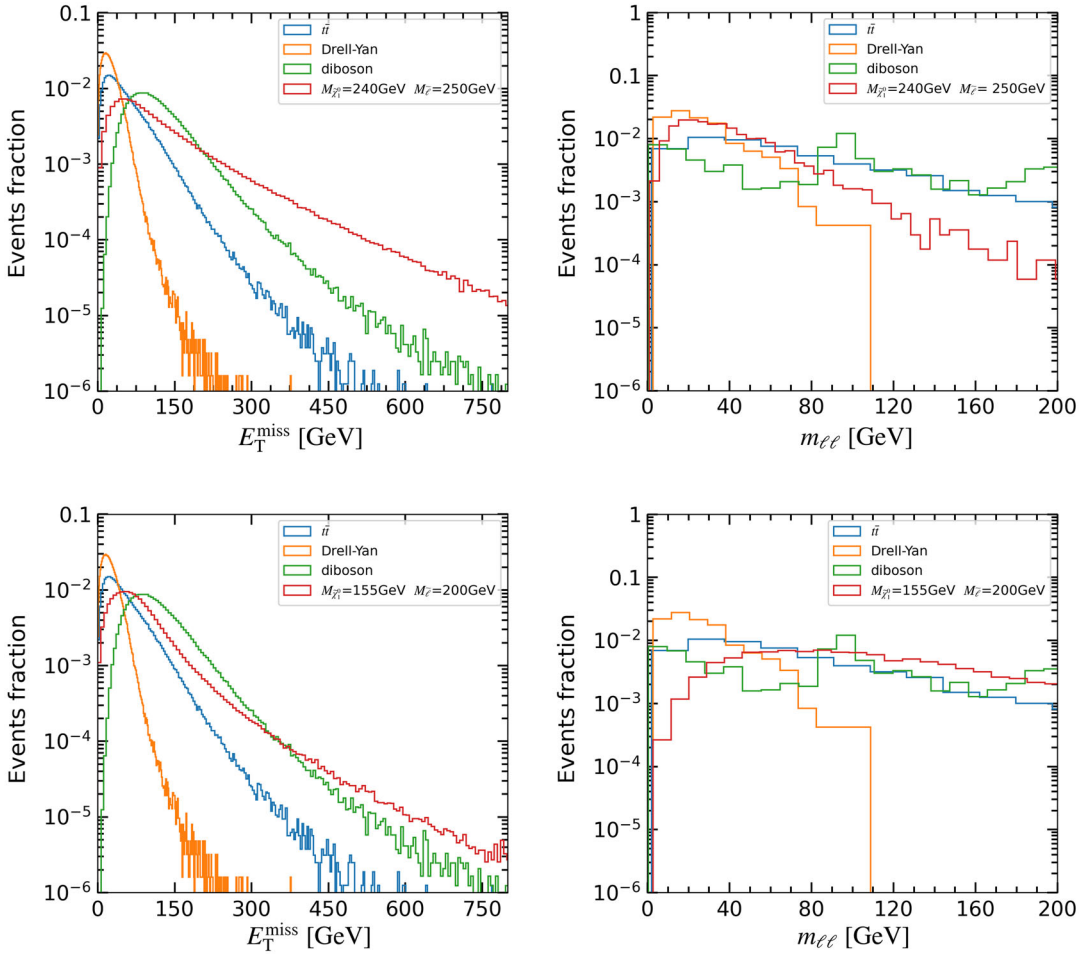

FIG. 7. The normalized $E_{\mathrm{T}}^{\mathrm{miss}}$ and $m_{\ell\ell}$ distributions of the signal and the SM background events at the 14 TeV HL-LHC. The upper and lower panels are for the final states with soft and hard 2ℓ, respectively.

TABLE I. The cut flows for the cross sections in units of fb at the 14 TeV HL-LHC. For the soft dilepton signal we choose a benchmark point $m_{\tilde{\chi}_1^0} = 240$ GeV, $m_{\tilde{\ell}} = 250$ GeV, $\tan\beta = 50$; while for the hard dilepton signal we choose a benchmark point $m_{\tilde{\chi}_1^0} = 155$ GeV, $m_{\tilde{\ell}} = 200$ GeV, $\tan\beta = 38.5$.

Soft Dilepton Channel				
	SM Backgrounds			Signal
Cuts	$t\bar{t}$	Diboson	Drell-Yan	(250, 240)
$E_{\mathrm{T}}^{\mathrm{miss}}$ Trigger	138727.9	5599.09	1565.4	12.05
Dilepton preselection	6041.48	361.02	104.95	4.57
ISR jet preselection	195.00	40.87	47.52	2.17
OSSF	82.26	20.08	6.93	1.96
Signal region	2.65	1.09	0.99	0.17

Hard Dilepton Channel				
	SM Backgrounds			Signal
Cuts	$t\bar{t}$	Diboson	Drell-Yan	(200, 155)
$N_\ell \geq 2, p_{\mathrm{T}}^{\ell_1} > 25$ GeV, $p_{\mathrm{T}}^{\ell_2} > 25$ GeV	20471.83	3622.38	16096.39	13.92
OSSF, $N_{b-\mathrm{jet}} = 0$	76.28	467.62	580.97	0.57
$m_{\ell\ell} > 121.2$ GeV	31.17	94.06	8.90	0.32
$E_{\mathrm{T}}^{\mathrm{miss}}$-significance > 10, $E_{\mathrm{T}}^{\mathrm{miss}} > 110$ GeV, $m_{\mathrm{T2}} > 100$ GeV	4.64	3.82	1.48	0.06

of the signal and background events. According to the kinematic features including those shown in Fig. 7, we impose the following event selection criteria.

For the soft dilepton plus missing energy channel, corresponding to the compressed mass spectrum, the event selection is optimized via Recursive Jigsaw Reconstruction technique [107,108] as follows:

Cut-1— $E_{\mathrm{T}}^{\mathrm{miss}}$ trigger. The first cut requires $E_{\mathrm{T}}^{\mathrm{miss}} > 110$ GeV.

Cut-2— Dilepton preselection. Before assigning visible objects to the jigsaw decay tree, the preselection criteria require the signal to have exactly two leptons with $p^{\ell_1} > 5$ GeV; the invariant mass $m_{\ell\ell}$ not in the range $[3.0, 3.2]$ GeV to remove contributions from J/ψ decays; $m_{\ell\ell}$ is further required to be smaller than 60 GeV to suppress the background from on-shell Z-boson decays. To reduce background events containing the so-called fake nonprompt leptons, the lepton pairs should be separated: $\Delta R_{\mu\mu} > 0.05$, $\Delta R_{ee} > 0.3$ and $\Delta R_{e\mu} > 0.2$.

Cut-3— ISR jet preselection. We require at least one jet with $p_{\mathrm{T}}^{j} > 110$ GeV as, for signal events, lepton pairs are boosted by energetic ISR jets. The leading jet is required to be on the different hemisphere from the missing momentum $\Delta\phi(j_1, \vec{p}_{\mathrm{T}}^{\mathrm{miss}}) > 2.0$, while the additional jets, which are assigned into the ISR system of the compressed decay tree, must satisfy $\Delta\phi(j, \vec{p}_{\mathrm{T}}^{\mathrm{miss}}) > 0.4$. Furthermore, events with b-tagging jets and $p_{\mathrm{T}}^{b-\mathrm{jet}} > 20$ GeV are vetoed.

Cut-4— OSSF. Signal events contain one opposite-sign same-flavor (OSSF) lepton pair plus large missing energy. And to suppress the Drell-Yan backgrounds $Z \to \tau\tau, \tau \to \ell\nu\nu$, the $m_{\tau\tau}$ variable, defined in [109–111], is required to be negative or to be greater than 160 GeV.

Cut-SR— Signal region. We require $E_{\mathrm{T}}^{\mathrm{miss}} > 200$ GeV. The transverse mass variable $m_{\mathrm{T2}}^{m_\chi}$ [112–114], with m_χ being an input mass variable, is used for finer signal selection. First, m_{T2}^{100} is required to be less than 140 GeV to improve the compressed spectrum, where the chosen value of $m_\chi = 100$ GeV is from Higgsino mass. Second, the m_{T2}^{100} distribution has an end point of 100 GeV and the difference $(m_{\mathrm{T2}}^{100} - 100)$ reflects the mass splitting between $\widetilde{\ell}$ and LSP, which is closely related to the lepton energy. So we require $p_{\mathrm{T}}^{\ell_2} > \min(20, 2.5 + 2.5 \times (m_{\mathrm{T2}}^{100} - 100))$. Finally, the R_{ISR} variable estimated by the Recursive Jigsaw Reconstruction technique, which approximately follows the relation $R_{\mathrm{ISR}} \sim m_{\tilde{\chi}_1^0}/m_{\widetilde{\ell}}$, is required that $\max(0.85, 0.98 - 0.02 \times m_{\mathrm{T2}}^{100}) < R_{\mathrm{ISR}} < 1$.

For the hard dilepton channel, the searching strategy is more straightforward. Signal events are required to have two OSSF leptons ℓ_1 and ℓ_2 with $p_{\mathrm{T}}^{\ell} > 25$ GeV and the invariant mass $m_{\ell\ell} > 121.2$ GeV. Any event that contains one b-tagging jet with $p_{\mathrm{T}} > 20$ GeV is removed to suppress the $t\bar{t}$ background. We also require a large missing transverse energy $E_{\mathrm{T}}^{\mathrm{miss}} > 110$ GeV and $E_{\mathrm{T}}^{\mathrm{miss}}$ significance > 10 [$E_{\mathrm{T}}^{\mathrm{miss}}$ significance is defined in Eq. (1) in [115]]. Finally, $m_{\mathrm{T2}} > 100$ GeV is required to reduce SM backgrounds further.

In Table I, we demonstrate the cut flows for the benchmark points in two channels. For both soft and hard

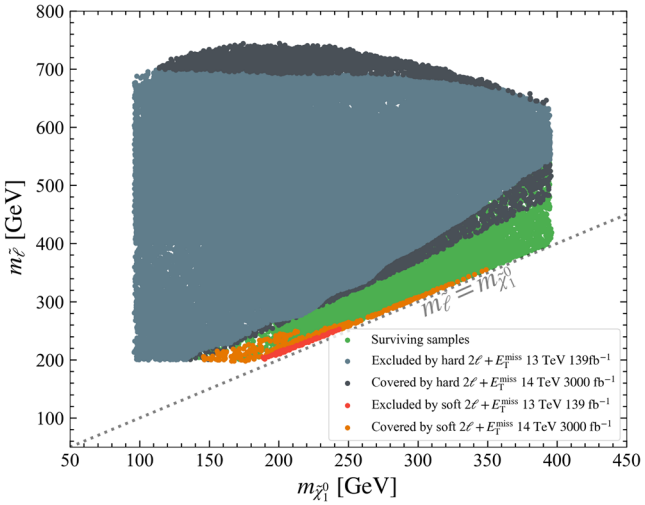

FIG. 8. Same as Fig. 4, but showing the detection limits of the processes $pp \to \tilde{\ell}\tilde{\ell}$ +jets at the HL-LHC.

dilepton channels, the cut on missing energy $E_{\mathrm{T}}^{\mathrm{miss}}$ is quite crucial to suppress backgrounds. To reduce the huge top pair background, the veto of b-jets is quite efficient. Finally, with all these cuts, we display in Fig. 8 the significance of the processes $pp \to j\tilde{\ell}^+\tilde{\ell}^-$ at the HL-LHC. We see that compared with the current LHC coverage, the HL-LHC can further cover a sizable part of the parameter space favored by the muon $g-2$ at 2σ level.

Note that we checked that in this light Higgsino scenario the contribution to the W-boson mass is quite small, much below the magnitude to explain the measured value by CDF II [116]. The reason is that, as found in [117], the SUSY contribution to the W-boson mass mainly comes from the stops and the explanation of CDF II result needs a stop around 1 TeV. In our scenario, stops are assumed to be quite heavy. Also, this light Higgsino scenario cannot jointly explain the electron and muon $g-2$ anomalies (with the fine structure constant from the Berkeley experiment [118], the SM value of electron $g-2$ is above the experimental value [119] by 2.4σ). As shown in [49,120–125], a joint explanation needs a rather special parameter space in SUSY.

V. CONCLUSIONS

We examined the light Higgsino scenario in light of the muon $g-2$ data. The dark matter constraints on the light Higgsino-like LSP were also taken into account. Assuming a light Higgsino mass parameter μ in the range of 100–400 GeV while keeping gaugino mass parameters above TeV, we explored the parameter space. We found that, to explain the muon $g-2$ anomaly at 2σ level, the winos and sleptons are respectively upper bounded by 3 TeV and 800 GeV. Then, for the light Higgsino-like LSP, we found that it can sizably scatter with nucleon and thus the allowed parameter space can be covered almost fully by the future LZ dark matter detection project. Finally, for the light leptons we performed a Monte Carlo simulation for their pair production at the HL-LHC and found that compared with the current LHC limits, the HL-LHC can further cover a sizable part of the parameter space.

ACKNOWLEDGMENTS

This work was supported by the National Natural Science Foundation of China under Grant No. 12275066 and by the startup research funds of Henan University.

[1] B. Abi, T. Albahri, S. Al-Kilani, D. Allspach, L. P. Alonzi, A. Anastasi *et al.* (Muon $g-2$ Collaboration), Measurement of the Positive Muon Anomalous Magnetic Moment to 0.46 ppm, Phys. Rev. Lett. **126**, 141801 (2021).
[2] G. W. Bennett *et al.* (Muon $g-2$ Collaboration), Final report of the E821 muon anomalous magnetic moment measurement at BNL, Phys. Rev. D **73**, 072003 (2006).
[3] T. Aoyama *et al.*, The anomalous magnetic moment of the muon in the Standard Model, Phys. Rep. **887**, 1 (2020).
[4] T. Blum, P. A. Boyle, V. Gülpers, T. Izubuchi, L. Jin, C. Jung, A. Jüttner, C. Lehner, A. Portelli, and J. T. Tsang (RBC and UKQCD Collaborations), Calculation of the Hadronic Vacuum Polarization Contribution to the Muon Anomalous Magnetic Moment, Phys. Rev. Lett. **121**, 022003 (2018).
[5] S. Weinberg, The cosmological constant problem, Rev. Mod. Phys. **61**, 1 (1989).
[6] G. Colangelo, A. X. El-Khadra, M. Hoferichter, A. Keshavarzi, C. Lehner, P. Stoffer, and T. Teubner, Data-driven evaluations of Euclidean windows to scrutinize hadronic vacuum polarization, Phys. Lett. B **833**, 137313 (2022).
[7] M. Cè *et al.*, Window observable for the hadronic vacuum polarization contribution to the muon $g-2$ from lattice QCD, Phys. Rev. D **106**, 114502 (2022).
[8] S. Borsanyi *et al.*, Leading hadronic contribution to the muon magnetic moment from lattice QCD, Nature (London) **593**, 51 (2021).
[9] C. T. H. Davies *et al.* (Fermilab Lattice, MILC, and HPQCD Collaborations), Windows on the hadronic vacuum polarization contribution to the muon anomalous magnetic moment, Phys. Rev. D **106**, 074509 (2022).
[10] C. Alexandrou *et al.*, Lattice calculation of the short and intermediate time-distance hadronic vacuum polarization

contributions to the muon magnetic moment using twisted-mass fermions, arXiv:2206.15084.
[11] M. Passera, W. J. Marciano, and A. Sirlin, The muon $g-2$ and the bounds on the Higgs boson mass, Phys. Rev. D **78**, 013009 (2008).
[12] A. Crivellin, M. Hoferichter, C. A. Manzari, and M. Montull, Hadronic Vacuum Polarization: $(g-2)_\mu$ Versus Global Electroweak Fits, Phys. Rev. Lett. **125**, 091801 (2020).
[13] G. Colangelo, M. Hoferichter, and P. Stoffer, Constraints on the two-pion contribution to hadronic vacuum polarization, Phys. Lett. B **814**, 136073 (2021).
[14] A. Keshavarzi, W. J. Marciano, M. Passera, and A. Sirlin, Muon $g-2$ and $\Delta\alpha$ connection, Phys. Rev. D **102**, 033002 (2020).
[15] F. Wang, W. Wang, J. Yang, Y. Zhang, and B. Zhu, Low energy supersymmetry confronted with current experiments: An overview, Universe **8**, 178 (2022).
[16] H. Baer, V. Barger, D. Sengupta, S. Salam, and K. Sinha, Status of weak scale supersymmetry after LHC Run 2 and ton-scale noble liquid WIMP searches, Eur. Phys. J. Special Topics **229**, 3085 (2020).
[17] J. M. Yang, P. Zhu, and R. Zhu, A brief survey of low energy supersymmetry under current experiments, Proc. Sci. LHCP2022 (**2022**) 069 [arXiv:2211.06686].
[18] T. Moroi, The muon anomalous magnetic dipole moment in the minimal supersymmetric standard model, Phys. Rev. D **53**, 6565 (1996).
[19] D. Stockinger, The muon magnetic moment and supersymmetry, J. Phys. G **34**, R45 (2007).
[20] S. P. Martin and J. D. Wells, Muon anomalous magnetic dipole moment in supersymmetric theories, Phys. Rev. D **64**, 035003 (2001).
[21] H. E. Haber and G. L. Kane, The search for supersymmetry: Probing physics beyond the Standard Model, Phys. Rep. **117**, 75 (1985).
[22] J. Cao, Z. Heng, D. Li, and J. M. Yang, Current experimental constraints on the lightest Higgs boson mass in the constrained MSSM, Phys. Lett. B **710**, 665 (2012).
[23] U. Ellwanger, C. Hugonie, and A. M. Teixeira, The next-to-minimal supersymmetric Standard Model, Phys. Rep. **496**, 1 (2010).
[24] J.-J. Cao, Z.-X. Heng, J. M. Yang, Y.-M. Zhang, and J.-Y. Zhu, A SM-like Higgs near 125 GeV in low energy SUSY: A comparative study for MSSM and NMSSM, J. High Energy Phys. 03 (2012) 086.
[25] M. Chakraborti, S. Heinemeyer, and I. Saha, Improved $(g-2)_\mu$ measurements and supersymmetry, Eur. Phys. J. C **80**, 984 (2020).
[26] M. Chakraborti, S. Heinemeyer, and I. Saha, Improved $(g-2)_\mu$ measurements and wino/Higgsino dark matter, Eur. Phys. J. C **81**, 1069 (2021).
[27] M. Chakraborti, S. Heinemeyer, and I. Saha, The new "MUON G-2" result and supersymmetry, Eur. Phys. J. C **81**, 1114 (2021).
[28] M. Chakraborti, S. Heinemeyer, and I. Saha, Improved $(g-2)_\mu$ measurements and supersymmetry: Implications for e^+e^- colliders, in *International Workshop on Future Linear Colliders*, arXiv:2105.06408.
[29] M. Chakraborti, S. Heinemeyer, and I. Saha, SUSY in the light of the new "MUON G-2" Result, Proc. Sci. EPS-HEP2021 (**2022**) 694 [arXiv:2111.00322].
[30] M. Chakraborti, S. Heinemeyer, I. Saha, and C. Schappacher, $(g-2)_\mu$ and SUSY dark matter: Direct detection and collider search complementarity, Eur. Phys. J. C **82**, 483 (2022).
[31] M. Chakraborti, S. Heinemeyer, and I. Saha, SUSY dark matter direct detection prospects based on $(g-2)_{\boldsymbol{\mu}}$, Moscow Univ. Phys. Bull. **77**, 116 (2022).
[32] M. Abdughani, K.-I. Hikasa, L. Wu, J. M. Yang, and J. Zhao, Testing electroweak SUSY for muon $g-2$ and dark matter at the LHC and beyond, J. High Energy Phys. 11 (2019) 095 [arXiv:1909.07792].
[33] P. Cox, C. Han, and T. T. Yanagida, Muon $g-2$ and dark matter in the minimal supersymmetric standard model, Phys. Rev. D **98**, 055015 (2018).
[34] P. Athron, C. Balázs, D. H. J. Jacob, W. Kotlarski, D. Stöckinger, and H. Stöckinger-Kim, New physics explanations of a_μ in light of the FNAL muon $g-2$ measurement, J. High Energy Phys. 09 (2021) 080 [arXiv:2104.03691].
[35] F. Wang, L. Wu, Y. Xiao, J. M. Yang, and Y. Zhang, GUT-scale constrained SUSY in light of new muon g-2 measurement, Nucl. Phys. **B970**, 115486 (2021).
[36] X. Ning and F. Wang, Solving the muon g-2 anomaly within the NMSSM from generalized deflected AMSB, J. High Energy Phys. 08 (2017) 089.
[37] M. Abdughani, Y.-Z. Fan, L. Feng, Y.-L. S. Tsai, L. Wu, and Q. Yuan, A common origin of muon g-2 anomaly, Galaxy Center GeV excess and AMS-02 anti-proton excess in the NMSSM, Sci. Bull. **66**, 2170 (2021).
[38] J. Cao, J. Lian, Y. Pan, D. Zhang, and P. Zhu, Improved $(g-2)_\mu$ measurement and singlino dark matter in μ-term extended Z_3-NMSSM, J. High Energy Phys. 09 (2021) 175.
[39] K. Wang and J. Zhu, Smuon in the NMSSM confronted with the muon $g-2$ anomaly and SUSY searches, Chin. Phys. C **47**, 013107 (2023).
[40] J. Cao, F. Li, J. Lian, Y. Pan, and D. Zhang, Impact of LHC probes of SUSY and recent measurement of $(g-2)_\mu$ on Z_3-NMSSM, Sci. China Phys. Mech. Astron. **65**, 291012 (2022).
[41] T.-P. Tang, M. Abdughani, L. Feng, Y.-L. S. Tsai, J. Wu, and Y.-Z. Fan, NMSSM neutralino dark matter for CDF II W-boson mass and muon $g-2$ and the promising prospect of direct detection, Sci. China Phys. Mech. Astron. **66**, 239512 (2023).
[42] J. Cao, Y. He, L. Shang, Y. Zhang, and P. Zhu, Current status of a natural NMSSM in light of LHC 13 TeV data and XENON-1T results, Phys. Rev. D **99**, 075020 (2019).
[43] J. Cao, J. Lian, Y. Pan, Y. Yue, and D. Zhang, Impact of recent $(g-2)_\mu$ measurement on the light CP-even Higgs scenario in general next-to-minimal supersymmetric Standard Model, J. High Energy Phys. 03 (2022) 203.
[44] J. Cao, X. Jia, L. Meng, Y. Yue, and D. Zhang, Status of the singlino-dominated dark matter in general next-to-minimal supersymmetric Standard Model, arXiv:2210.08769.

[45] S.-M. Zhao, L.-H. Su, X.-X. Dong, T.-T. Wang, and T.-F. Feng, Study muon $g-2$ at two-loop level in the $U(1)_X$SSM, J. High Energy Phys. 03 (2022) 101.
[46] J.-L. Yang, H.-B. Zhang, C.-X. Liu, X.-X. Dong, and T.-F. Feng, Muon $(g-2)$ in the B-LSSM, J. High Energy Phys. 08 (2021) 086.
[47] H.-B. Zhang, C.-X. Liu, J.-L. Yang, and T.-F. Feng, Muon anomalous magnetic dipole moment in the $\mu\nu$SSM *, Chin. Phys. C **46**, 093107 (2022).
[48] J. Cao, J. Lian, L. Meng, Y. Yue, and P. Zhu, Anomalous muon magnetic moment in the inverse seesaw extended next-to-minimal supersymmetric Standard Model, Phys. Rev. D **101**, 095009 (2020).
[49] J. Cao, Y. He, J. Lian, D. Zhang, and P. Zhu, Electron and muon anomalous magnetic moments in the inverse seesaw extended NMSSM, Phys. Rev. D **104**, 055009 (2021).
[50] X. Wang, S.-M. Zhao, X.-X. Long, Y.-T. Wang, T.-T. Wang, H.-B. Zhang *et al.*, Study on muon MDM and lepton EDM in BLMSSM via the mass insertion approximation, arXiv:2211.10848.
[51] T. Li, J. Pei, and W. Zhang, Muon anomalous magnetic moment and Higgs potential stability in the 331 model from SU(6), Eur. Phys. J. C **81**, 671 (2021).
[52] R. K. Barman, G. Bélanger, B. Bhattacherjee, R. M. Godbole, and R. Sengupta, Is the light neutralino thermal dark matter in the MSSM ruled out?, arXiv:2207.06238.
[53] M. Chakraborti, L. Roszkowski, and S. Trojanowski, GUT-constrained supersymmetry and dark matter in light of the new $(g-2)_\mu$ determination, J. High Energy Phys. 05 (2021) 252.
[54] A. Aboubrahim, P. Nath, and R. M. Syed, Yukawa coupling unification in an SO(10) model consistent with Fermilab $(g-2)_\mu$ result, J. High Energy Phys. 06 (2021) 002.
[55] B. Zhu, R. Ding, and T. Li, Higgs mass and muon anomalous magnetic moment in the MSSM with gauge-gravity hybrid mediation, Phys. Rev. D **96**, 035029 (2017).
[56] S. Akula and P. Nath, Gluino-driven radiative breaking, Higgs boson mass, muon $g-2$, and the Higgs diphoton decay in supergravity unification, Phys. Rev. D **87**, 115022 (2013).
[57] Z. Li, G.-L. Liu, F. Wang, J. M. Yang, and Y. Zhang, Gluino-SUGRA scenarios in light of FNAL muon g-2 anomaly, J. High Energy Phys. 12 (2021) 219.
[58] F. Wang, W. Wang, and J. M. Yang, Reconcile muon g-2 anomaly with LHC data in SUGRA with generalized gravity mediation, J. High Energy Phys. 06 (2015) 079.
[59] F. Wang, K. Wang, J. M. Yang, and J. Zhu, Solving the muon g-2 anomaly in CMSSM extension with non-universal gaugino masses, J. High Energy Phys. 12 (2018) 041.
[60] W. Ahmed, I. Khan, J. Li, T. Li, S. Raza, and W. Zhang, The natural explanation of the muon anomalous magnetic moment via the electroweak supersymmetry from the GmSUGRA in the MSSM, Phys. Lett. B **827**, 136879 (2022).
[61] Z. Kang, T. Li, T. Liu, C. Tong, and J. M. Yang, A heavy SM-like Higgs and a light stop from Yukawa-deflected gauge mediation, Phys. Rev. D **86**, 095020 (2012).
[62] J. L. Evans, M. Ibe, S. Shirai, and T. T. Yanagida, A 125 GeV Higgs boson and muon $g-2$ in more generic gauge mediation, Phys. Rev. D **85**, 095004 (2012).
[63] F. Wang, W. Wang, J. M. Yang, and Y. Zhang, Heavy colored SUSY partners from deflected anomaly mediation, J. High Energy Phys. 07 (2015) 138.
[64] F. Wang, J. M. Yang, and Y. Zhang, Radiative natural SUSY spectrum from deflected AMSB scenario with messenger-matter interactions, J. High Energy Phys. 04 (2016) 177.
[65] J. L. Lamborn, T. Li, J. A. Maxin, and D. V. Nanopoulos, Resolving the $(g-2)_\mu$ discrepancy with $\mathcal{F}-SU(5)$ intersecting D-branes, J. High Energy Phys. 11 (2021) 081.
[66] S. Iwamoto, T. T. Yanagida, and N. Yokozaki, Wino-Higgsino dark matter in MSSM from the $g-2$ anomaly, Phys. Lett. B **823**, 136768 (2021).
[67] X. Tata, Natural supersymmetry: Status and prospects, Eur. Phys. J. Special Topics **229**, 3061 (2020).
[68] R. L. Arnowitt and P. Nath, Loop corrections to radiative breaking of electroweak symmetry in supersymmetry, Phys. Rev. D **46**, 3981 (1992).
[69] C. Han, A. Kobakhidze, N. Liu, A. Saavedra, L. Wu, and J. M. Yang, Probing light Higgsinos in natural SUSY from monojet signals at the LHC, J. High Energy Phys. 02 (2014) 049.
[70] P. Athron *et al.* (GAMBIT Collaboration), Combined collider constraints on neutralinos and charginos, Eur. Phys. J. C **79**, 395 (2019).
[71] T. Buanes, I. Lara, K. Rolbiecki, and K. Sakurai, LHC constraints on electroweakino dark matter revisited, arXiv:2208.04342.
[72] A. Djouadi, M. M. Muhlleitner, and M. Spira, Decays of supersymmetric particles: The program SUSY-HIT (SuSpect-SdecaY-Hdecay-InTerface), Acta Phys. Pol. B **38**, 635 (2007).
[73] G. Degrassi, S. Heinemeyer, W. Hollik, P. Slavich, and G. Weiglein, Towards high precision predictions for the MSSM Higgs sector, Eur. Phys. J. C **28**, 133 (2003).
[74] H. Bahl, S. Heinemeyer, W. Hollik, and G. Weiglein, Theoretical uncertainties in the MSSM Higgs boson mass calculation, Eur. Phys. J. C **80**, 497 (2020).
[75] E. Bagnaschi, J. Pardo Vega, and P. Slavich, Improved determination of the Higgs mass in the MSSM with heavy superpartners, Eur. Phys. J. C **77**, 334 (2017).
[76] P. Athron, J.-h. Park, T. Steudtner, D. Stöckinger, and A. Voigt, Precise Higgs mass calculations in (non-)minimal supersymmetry at both high and low scales, J. High Energy Phys. 01 (2017) 079.
[77] B. C. Allanach, A. Djouadi, J. L. Kneur, W. Porod, and P. Slavich, Precise determination of the neutral Higgs boson masses in the MSSM, J. High Energy Phys. 09 (2004) 044
[78] I. Gogoladze, Q. Shafi, and C. S. Un, Higgs boson mass from t-b-τ Yukawa unification, J. High Energy Phys. 08 (2012) 028.
[79] M. Adeel Ajaib, I. Gogoladze, Q. Shafi, and C. S. Un, A predictive Yukawa unified SO(10) model: Higgs and sparticle masses, J. High Energy Phys. 07 (2013) 139.
[80] P. Drechsel, R. Gröber, S. Heinemeyer, M. M. Muhlleitner, H. Rzehak, and G. Weiglein, Higgs-boson masses and

mixing matrices in the NMSSM: Analysis of on-shell calculations, Eur. Phys. J. C **77**, 366 (2017).
[81] D. Chowdhury, R. M. Godbole, K. A. Mohan, and S. K. Vempati, Charge and color breaking constraints in MSSM after the Higgs discovery at LHC, J. High Energy Phys. 02 (2014) 110.
[82] G. Belanger, F. Boudjema, P. Brun, A. Pukhov, S. Rosier-Lees, P. Salati, and A. Semenov, Indirect search for dark matter with micrOMEGAs2.4, Comput. Phys. Commun. **182**, 842 (2011).
[83] N. Aghanim *et al.* (Planck Collaboration), Planck 2018 results. VI. Cosmological parameters, Astron. Astrophys. **641**, A6 (2020).
[84] P. Athron, M. Bach, H. G. Fargnoli, C. Gnendiger, R. Greifenhagen, J.-h. Park, S. Paßehr, D. Stöckinger, H. Stöckinger-Kim, and A. Voigt, GM2Calc: Precise MSSM prediction for $(g-2)$ of the muon, Eur. Phys. J. C **76**, 62 (2016).
[85] P. Athron, C. Balazs, A. Cherchiglia, D. H. J. Jacob, D. Stoeckinger, H. Stoeckinger-Kim *et al.*, GM2Calc—2 for the 2HDM, Proc. Sci. CompTools2021 (**2022**) 009.
[86] B. Abi *et al.* (Muon $g-2$ Collaboration), Measurement of the Positive Muon Anomalous Magnetic Moment to 0.46 ppm, Phys. Rev. Lett. **126**, 141801 (2021).
[87] P. von Weitershausen, M. Schafer, H. Stockinger-Kim, and D. Stockinger, Photonic SUSY two-loop corrections to the muon magnetic moment, Phys. Rev. D **81**, 093004 (2010).
[88] H. Fargnoli, C. Gnendiger, S. Paßehr, D. Stöckinger, and H. Stöckinger-Kim, Two-loop corrections to the muon magnetic moment from fermion/sfermion loops in the MSSM: Detailed results, J. High Energy Phys. 02 (2014) 070.
[89] M. Bach, J.-h. Park, D. Stöckinger, and H. Stöckinger-Kim, Large muon $(g-2)$ with TeV-scale SUSY masses for $\tan\beta \to \infty$, J. High Energy Phys. 10 (2015) 026.
[90] G. Aad *et al.* (ATLAS Collaboration), Search for electroweak production of charginos and sleptons decaying into final states with two leptons and missing transverse momentum in $\sqrt{s} = 13$ TeV pp collisions using the ATLAS detector, Eur. Phys. J. C **80**, 123 (2020).
[91] G. Aad *et al.* (ATLAS Collaboration), Searches for electroweak production of supersymmetric particles with compressed mass spectra in $\sqrt{s} = 13$ TeV pp collisions with the ATLAS detector, Phys. Rev. D **101**, 052005 (2020).
[92] A. Reinert and M. W. Winkler, A precision search for WIMPs with charged cosmic rays, J. Cosmol. Astropart. Phys. 01 (2018) 055.
[93] D. S. Akerib *et al.* (LUX Collaboration), Limits on Spin-Dependent WIMP-Nucleon Cross Section Obtained from the Complete LUX Exposure, Phys. Rev. Lett. **118**, 251302 (2017).
[94] E. Aprile *et al.* (XENON Collaboration), Dark Matter Search Results from a One Ton-Year Exposure of XENON1T, Phys. Rev. Lett. **121**, 111302 (2018).
[95] E. Aprile *et al.* (XENON Collaboration), Constraining the Spin-Dependent WIMP-Nucleon Cross Sections with XENON1T, Phys. Rev. Lett. **122**, 141301 (2019).
[96] J. Xia *et al.* (PandaX-II Collaboration), PandaX-II constraints on spin-dependent WIMP-nucleon effective interactions, Phys. Lett. B **792**, 193 (2019).
[97] Y. Meng *et al.* (PandaX-4T Collaboration), Dark Matter Search Results from the PandaX-4T Commissioning Run, Phys. Rev. Lett. **127**, 261802 (2021).
[98] J. Aalbers *et al.* (LZ Collaboration), First dark matter search results from the LUX-ZEPLIN (LZ) experiment, arXiv:2207.03764.
[99] D. S. Akerib *et al.* (LZ Collaboration), Projected WIMP sensitivity of the LUX-ZEPLIN dark matter experiment, Phys. Rev. D **101**, 052002 (2020).
[100] E. Aprile *et al.* (XENON Collaboration), Projected WIMP sensitivity of the XENONnT dark matter experiment, J. Cosmol. Astropart. Phys. 11 (2020) 031.
[101] J. Alwall, R. Frederix, S. Frixione, V. Hirschi, F. Maltoni, O. Mattelaer, H.-S. Shao, T. Stelzer, P. Torrielli, and M. Zaro, The automated computation of tree-level and next-to-leading order differential cross sections, and their matching to parton shower simulations, J. High Energy Phys. 07 (2014) 079.
[102] T. Sjöstrand, S. Ask, J. R. Christiansen, R. Corke, N. Desai, P. Ilten, S. Mrenna, S. Prestel, C. O. Rasmussen, and P. Z. Skands, An introduction to PYTHIA 8.2, Comput. Phys. Commun. **191**, 159 (2015).
[103] J. de Favereau, C. Delaere, P. Demin, A. Giammanco, V. Lemaître, A. Mertens, and M. Selvaggi (Delphes 3 Collaboration), Delphes 3, A modular framework for fast simulation of a generic collider experiment, J. High Energy Phys. 02 (2014) 057.
[104] M. Drees, H. Dreiner, J. S. Kim, D. Schmeier, and J. Tattersall, CheckMATE: Confronting your favourite new physics model with LHC data, Comput. Phys. Commun. **187**, 227 (2015).
[105] J. S. Kim, D. Schmeier, J. Tattersall, and K. Rolbiecki, A framework to create customised LHC analyses within CheckMATE, Comput. Phys. Commun. **196**, 535 (2015).
[106] D. Dercks, N. Desai, J. S. Kim, K. Rolbiecki, J. Tattersall, and T. Weber, CheckMATE 2: From the model to the limit, Comput. Phys. Commun. **221**, 383 (2017).
[107] P. Jackson, C. Rogan, and M. Santoni, Sparticles in motion: Analyzing compressed SUSY scenarios with a new method of event reconstruction, Phys. Rev. D **95**, 035031 (2017).
[108] P. Jackson and C. Rogan, Recursive Jigsaw reconstruction: HEP event analysis in the presence of kinematic and combinatoric ambiguities, Phys. Rev. D **96**, 112007 (2017).
[109] Z. Han, G. D. Kribs, A. Martin, and A. Menon, Hunting quasidegenerate Higgsinos, Phys. Rev. D **89**, 075007 (2014).
[110] H. Baer, A. Mustafayev, and X. Tata, Monojet plus soft dilepton signal from light Higgsino pair production at LHC14, Phys. Rev. D **90**, 115007 (2014).
[111] A. Barr and J. Scoville, A boost for the EW SUSY hunt: Monojet-like search for compressed sleptons at LHC14 with 100 fb^{-1}, J. High Energy Phys. 04 (2015) 147.
[112] C. Lester and A. Barr, MTGEN: Mass scale measurements in pair-production at colliders, J. High Energy Phys. 12 (2007) 102.

[113] C. G. Lester and D. J. Summers, Measuring masses of semi-invisibly decaying particle pairs produced at hadron colliders, Phys. Lett. B **463**, 99 (1999).
[114] A. Barr, C. G. Lester, and P. Stephens, A variable for measuring masses at hadron colliders when missing energy is expected; m_{T2}: The truth behind the glamour, J. Phys. G **29**, 2343 (2003).
[115] ATLAS Collaboration, Object-based missing transverse momentum significance in the ATLAS detector, CERN Technical Report No. ATLAS-CONF-2018-038, 2018.
[116] T. Aaltonen *et al.* (CDF Collaboration), High-precision measurement of the W boson mass with the CDF II detector, Science **376**, 170 (2022).
[117] J. M. Yang and Y. Zhang, Low energy SUSY confronted with new measurements of W-boson mass and muon $g-2$, Sci. Bull. **67**, 1430 (2022).
[118] R. H. Parker, C. Yu, W. Zhong, B. Estey, and H. Müller, Measurement of the fine-structure constant as a test of the Standard Model, Science **360**, 191 (2018).
[119] D. Hanneke, S. Fogwell, and G. Gabrielse, New Measurement of the Electron Magnetic Moment and the Fine Structure Constant, Phys. Rev. Lett. **100**, 120801 (2008).
[120] S. Li, Y. Xiao, and J. M. Yang, Can electron and muon $g-2$ anomalies be jointly explained in SUSY?, Eur. Phys. J. C **82**, 276 (2022).
[121] S. Li, Z. Li, F. Wang, and J. M. Yang, Explanation of electron and muon $g-2$ anomalies in AMSB, Nucl. Phys. **B983**, 115927 (2022).
[122] B. Dutta and Y. Mimura, Electron $g-2$ with flavor violation in MSSM, Phys. Lett. B **790**, 563 (2019).
[123] M. Endo and W. Yin, Explaining electron and muon $g-2$ anomaly in SUSY without lepton-flavor mixings, J. High Energy Phys. 08 (2019) 122.
[124] M. I. Ali, M. Chakraborti, U. Chattopadhyay, and S. Mukherjee, Muon and electron $(g-2)$ anomalies with non-holomorphic interactions in MSSM, Eur. Phys. J. C **83**, 60 (2023).
[125] J.-L. Yang, T.-F. Feng, and H.-B. Zhang, Electron and muon $(g-2)$ in the B-LSSM, J. Phys. G **47**, 055004 (2020).